

Self-Supervised Image Denoising Methods: an Application in Fetal MRI

Ana Cláudia Souza Vidal de Negreiros¹, Gilson Giraldi², Heron Werner³, Ítalo Messias Feliz Santos⁴

¹Federal Rural University of the Semi-Arid (UFERSA), Mossoró, Brazil

^{2,4}National Laboratory for Cientific Computing (LNCC), Petrópolis, Brazil

³Biodesign Lab Dasa/PUC-Rio de Janeiro, Brazil

anaclaudia.negreiros@ufersa.edu.br¹

Abstract - The process of image denoising in magnetic resonance imaging (MRI) is more and more common and important in the medical area. However, it is usual that state-of-the-art deep learning methods require pair images (clean and noisy ones) to train the models which poses limitations in practice. In this sense, this work applied two recent techniques that do not need a clean image to train the models and reached good results for denoising tasks. We applied the NOISE2NOISE (N2N) and the NOISE2VOID (N2V) learning approaches and compared the results for denoising tasks using a fetal MRI dataset. The results showed that the N2N method outperformed the N2V one, considering the Peak Signal-to-Noise Ratio (PSNR), Root Mean Squared Error (RMSE) evaluation metrics, and visual analysis.

Keywords—image denoising, medical area, NOISE2NOISE, NOISE2VOID, fetal MRI

I. INTRODUCTION

In the modern world, it is more and more usual to infer information from images. The Artificial Intelligence (AI) area has been a revolutionary way for classification, regression, anomaly detection, and other tasks in image databases. In this context, image denoising plays a vital space in the image processing field, with important goals especially in the medical areas [1], [2].

Image denoising is a well-known and important inverse problem in image processing and computer vision [3] and it has remained an essential problem in the field of medical image processing [4]. Indeed, medical image analysis involves accurate interpretation of image data for the proper diagnosis to decide further course of treatment [5]. Consequently, improving the quality of a medical image could mean higher odds of early disease detection by visual analysis.

However, state-of-the-art methods require, in general, pair images (clean and noisy ones) to train the models which represents another problem because it is very difficult, in many cases, to obtain a pair of clean and noisy images. This is particularly true for fetal MRI since it is not possible to ensure that the fetus will not move during the image acquisition process. Moreover, acquiring noise and clean data consumes financial and hardware resources being uncomfortable for the patient that should follow the acquisition protocol in two distinct times.

- This work reviews recent papers that applied both N2N and N2V methods for different tasks and in different fields.
- We show that it is possible to train a self-supervised methods (N2N and N2V) and to reach reasonable results considering the original models and a fetal MRI dataset without data augmentation.

To handle this drawback, it is possible to apply methods that do not need a respective clean image, only the noisy one, or self-supervised techniques such as NOISE2NOISE (N2N) [6] and NOISE2VOID (N2V) [7] approaches. The N2N method was proposed by Lehtinen et al. [6] in 2018 and instead of training a Convolutional Neural network (CNN) to map noisy inputs to clean ground truth images its training tries to learn a mapping between pairs of independently degraded versions of the same training image, i.e., $(s^j + n^j, s^j + n'^j)$, that incorporate the same signal s^j , but independently drawn zero-mean noise n^j and n'^j . As proved by Lehtinen et al. [6], a specific deep network trained to predict one noisy signal from an independent noisy measurement of the same signal will learn to predict the clean data. Thus, in cases where there are no pairs of images (clean and noisy ones), N2N can still qualify the training of denoising networks. Regardless of that advantage, in general, there are at least two shortcomings to this approach: (i) N2N training requires that two images capturing the same content (s^j) with independent noises (n^j, n'^j) are available, and (ii) the acquisition of such pairs with (quasi) constant s^j is only possible for (quasi) static scenes.

In this sense, there is the NOISE2VOID (N2V), a method designed to handle the N2N drawbacks. As N2N, also N2V supports the observation that high-quality denoising models can be trained without the availability of clean ground truth data. Nevertheless, unlike N2N or traditional training, N2V can also be applied to data for which neither noisy image pairs nor clean target images are available, i.e. N2V is a self-supervised training method. N2V makes two statistical assumptions: (i) the signal s is not pixel-wise independent, (ii) the noise n is conditionally pixel-wise independent given the signal s^j .

The objective of this work is to apply specific image-denoising methods that do not require ground truth images. These methods are the N2N and the N2V and they will be applied to a fetal magnetic resonance imaging (MRI) dataset. Also, we will compare N2N and N2V results through visual analysis and by computing the peak signal-to-noise ratio (PSNR) and root mean squared error (RMSE). Taking this into consideration, the main contributions of this research are the following:

The rest of this work is organized as follows. Section II brings the recent related works that apply both N2N and N2V. Section III addresses the two applied methods, N2N and N2V. Section IV presents the used MRI fetal image dataset. Section V details and compares the results obtained by applying N2N and N2V self-supervised methods. Finally, Section VI concludes the work with the main found results.

II. RELATED WORKS

Many studies have been carried out for image denoising to reach better quality images. In this context, self-supervised methods have also gained attention in this field. To analyze articles that applied N2N and N2V, we performed a search in the SCOPUS database and considered only recent papers to show that it is a modern subject.

Zharov et al [8] recently proposed the application of a N2N based method in radiographic and tomographic multichannel imaging, demonstrating applicability in this kind of image. Houhou et al. [9], in the context of biophonic multimodel imaging, compared the potential of N2N with other deep models in improving image quality. Jung et al. [10] also applied a smooth alteration in the N2N model and applied their method in 3D magnetic resonance images, with qualitative and quantitative evaluations. Besides, Jurek et al. [11] applied a N2N based model in diffusion magnetic resonance images (dMRI) also aiming to improve the denoising task in this type of neuroimaging. Batson and Royer [12] also proposed a N2N based denoiser that requires no prior on the signal, no estimate of the noise and no cleaning training data, where the optimal model for a given dataset is obtained by minimizing a self-supervised loss over a class of invariant functions. On the other hand, Ashwini and Ramashri [13] applied both N2N and N2V to chest X-ray images to identify COVID-19, once these two methods can give better quality images, facilitating the diagnosis. Lesage et al. [14] integrated N2V with another deep model aiming to analyze 3D images of ovaries. Besides, Yun et al. [15] proposed enhanced N2V that uses the total variation term to further denoise the images while preserving the essential details of computed tomography (CT) imagery. Also, kojima et al. [16] applied N2V in MRI, however, they tried to remove the noise of kiwi fruit, which is a fruit appropriate for evaluating spatial resolution and image contrast because of its fine structure and many components.

In this sense, the main difference between our work and counterpart ones is that we do not perform modifications in the original N2N and N2V models, we do not apply data augmentation, and our work has a specific application in a fetal MRI dataset.

III. DATASET

In this work, we used an MRI dataset, generated from 38 different patients (pregnant). MRI datasets has been widely used in the medical area, once, in general, it is composed of high-resolution images[17]. The dataset used in this work is not available to the public. A 1.5 – T scanner (Magnetom Aera, Siemens, Erlangen, Germany) performed the MRI examination, with the surface coil positioned on the abdomen. It was applied a 3D T2-weighted true fast imaging sequence with steady-state precession (truefisp) in sagittal plane ($TR/TE = 3.02/1.43ms$); besides, following isotropic voxel ($1.0 \times 1.0 \times 1.0mm^3$); matrix: $256 \times 256mm^2$, 136 slices, with a total acquisition time of 26s. Also, maternal sedation was not used in the patients.

To acquire the MRI dataset, the pregnant was positioned in dorsal or left lateral decubitus, with the feet entering the magnet first. Then, the images were acquired using a controlled setup with image acquisition during maternal breath-hold to produce high-quality images with low levels of artifacts/noise. During the capture of fetal MRI, it is not possible to prevent the movement of the fetus. So, it is not guaranteed that images obtained in a controlled environment

will be free of artifacts due to fetal movements.

For this study, synthetic images were created to compose the pairs of images (clean and noisy ones). In this sense, the additive Gaussian noise [18] was applied to the clean images. Thus, it was possible to compute some image quality metrics (PSNR and RMSE). The additive Gaussian noise is widely used in many contexts to create noisy images and to train different models for different fields and tasks. Fig. 1 shows a pair of clean and noisy fetal image. The clean one is from our dataset described above, and the noisy one was generated by additive Gaussian noise with standard deviation $\sigma = 20$. Also, we did not use data augmentation in this work because it was not in our initial scope, however, we intend to perform tests using augmented data in further research.

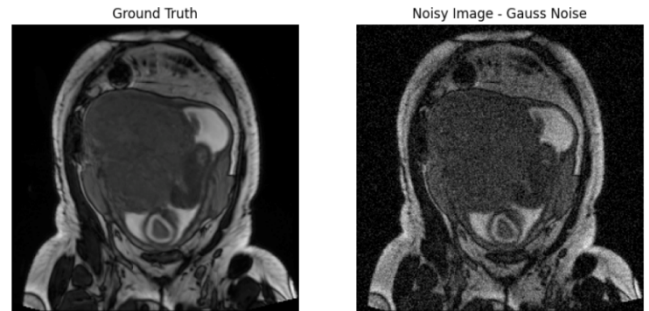


Fig. 1. Representation of clean (ground truth – left side) and a noisy image (right side). This noisy image was generated by using additive Gaussian noise.

IV. NOISE2NOISE AND NOISE2VOID NETWORKS

The N2N is an unsupervised deep learning model, which does not require clean images to train the network method. However, it requires the noisy measurements $s^j + n^j$ and $s^j + n'^j$ based on the true value s^j , with n^j and n'^j being zero-mean additive noises. The following expression represents the N2N method:

$$\operatorname{argmin}(\theta) = \sum_j L \left(f_\theta \left((s^j, n^j) \right), (s^j, n'^j) \right), \quad (1)$$

where f_θ is a parametric family of mappings under the loss function L . The key idea is that, with expression (1), N2N can learn to remove noise from a signal rather than learn from noise $s^j + n^j$ to noise $s^j + n'^j$. This is the principle of the N2N unsupervised method. Also, the key to this occurrence lies in the fact that the expected value of the noisy input is equal to the clean signal [6].

The architecture of N2N is a U-Net developed by Ronneberger et al. [19]. Also, it can be seen in the Appendix Section of Lehtinen et al. [6]. For all basic noise, the number of input and output channels was equal to 3.

The N2V method [7] relies on the fact, as the authors explain, that in a blind-spot network, the receptive field of each pixel excludes the pixel itself, preventing it from learning its identity. The authors show that this kind of network can learn to remove pixel-wise independent noise when they are trained on the same noisy images as input and target.

To understand the main difference between N2N and N2V first, it is important to see the pairs of noisy images used to train N2N as

$$x^j = (s^j, n^j) \text{ and } x'^j = (s^j, n'^j), \quad (2)$$

that is the two training images are identical up to their noise components n^j and n'^j . In the N2V case, these noises are in

the image generation by all input pixels in a square neighborhood except for the input pixel x_i at its very location. Authors call this type of network a blind-spot network. Also, a blind-spot network can be trained using a clean target or a noisy target, depending on the desired goal.

According to Krull et al. [7], the main advantage of a blind-spot network is its inability to learn the identity. In other words, since they assume the noise to be pixel-wise independent given the signal, the neighboring pixels carry no information about the value of n_i (noise). Thus, it is impossible for the network to produce an estimate that is better than a priori expected value. However, the signal is assumed to contain statistical dependencies. As a result, the network can still estimate the signal s_i of a pixel by looking at its surroundings. Hence, the N2V allows the extraction of the input patch and target value from the same noisy training image. Also, as in N2N (Eq. 1), the objective is to minimize the loss function or empirical risk. The N2V also applies a U-Net [19] but with addition of batch normalization [20] before each activation function.

V. COMPARISON AND DISCUSSION

The dataset (described in Section III) contains 2590 images, where 80% were used for training, 10% as validation set, and other 10% were used to test.

To apply the N2N and N2V methods, we add Gaussian noisy in the original images. Specifically, for N2N model, the training and validation sets is composed by pairs $(s^j + n^j, s^j + n^j)$ where s^j is the original image, and n^j and n'^j are generated by a Gaussian distribution with $\sigma = 20$ and zero-mean. The test set is formed by triplets $(s^j, s^j + n^j, s^j + n'^j)$ and the inference I^j is given by:

$$I^j = \frac{N2N(s^j+n^j)+N2N(s^j+n'^j)}{2}. \quad (3)$$

For N2V, the training and validation sets are composed single noisy images $(s^j + n^j)$ where s^j and n^j are analogous to N2N. The test is composed by pairs $(s^j, s^j + n^j)$ and the inference I^j is given by N2V($s^j + n^j$).

We ran the codes in Python, using PyTorch [21] for N2N and TensorFlow [22] and Keras [23] for N2V. The codes for N2N and N2V can be found in [6] and [7], respectively. Also, we did not use transfer learning in our training process, indeed, the N2V models do not allow us to save checkpoints during training.

In this sense, the networks weights were initialized following He et al. [24], they proposed a robust initialization method that removes an obstacle of training very deep networks. Besides, we also used the same hyperparameter values used in [6] to train the N2N model, and the same hyperparameter values applied in [7] to train the N2V network. Thus, to train the N2N no batch normalization, dropout, or other regularization techniques were used. Also, the training process applied the learning rate optimization ADAM [25] with parameters $\beta_1 = 0.9$ and $\beta_2 = 0.9$ and $\epsilon = 10^{-8}$. Also, a learning rate of 0.0001 was used and kept at a constant value during the training process. The two models were trained using 150 epochs.

On the other hand, to train N2V we randomly extract patches of size 64×64 . Within each patch N pixels were randomly selected, using stratified sampling to avoid clustering. Besides, the U-Net kernel size was 3 and the mean

square error (MSE) was the train loss function applied. For more information, see supplementary material made available by [7]. Results from the tests are shown in Figs 2 and 3. Besides, Table I presents evaluation metric results for both approaches. Also, the code was run in a GPU Tesla T4 with 16GB of GDDR6 memory and 2560 CUDA cores.

In this context, we used PSNR, and RMSE to evaluate the results of both methods. The formulas to compute these image quality metrics are given below.

$$PSNR = 20\log(MAX_I) - 10\log(MSE). \quad (4)$$

In the above formula, MAX_I is the maximum pixel value of image I and MSE (Eq. 5) is the mean squared error that considers the “true” numeric values for comparison between actual and degraded image [26].

$$MSE = \frac{1}{M \times N} \sum_{i=1}^M \sum_{j=1}^N [g(i, j) - f(i, j)]^2, \quad (5)$$

where M and N are the pixel amounts in the x direction and y direction, respectively, of the thin section images, and $g(i, j)$ and $f(i, j)$ are the grey values of the original thin section image and the cleaned thin section image, respectively, at point (i, j) .

The RMSE, another quality measure used in this paper, is defined as:

$$RMSE(g, f) = \sqrt{MSE}, \quad (6)$$

where MSE was defined in Eq. (5), g is the original signal, and f is the denoised signal.

In Fig. 2 and Fig. 3 it is presented the results for images 1 and 2, considering N2N and N2V methods. In both cases, the figures present clean, noisy (generated by additive Gaussian noise), and denoised images (generated by N2V and N2N). Also, in the two situations, it is possible to affirm that the denoising models were able to perform a noise reduction considering the noisy images. Besides, by visual analysis, it is also possible to affirm that N2N was better than N2V in terms of similarity between the clean image and the ground truth. However, there is a place to have better results considering the clean image. In other words, it is possible to improve the denoising performances for both tested images.

Besides Table I summarizes the quantitative results of both methods. This table presents the image quality metrics, in terms of the mean, for both methods (PSNR and RMSE). The quantitative results are important to make accurate conclusions about the results. In this case, Table I confirms the visual perception that N2N outperforms N2V in this test.

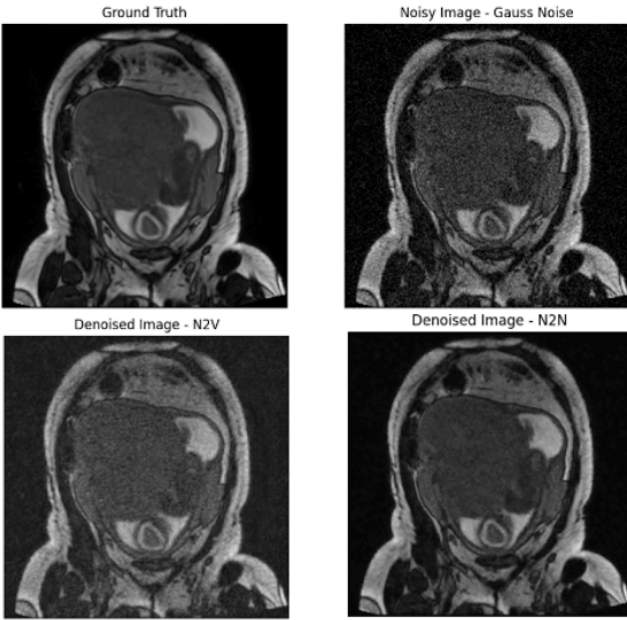


Fig. 2. Representation of one clean image (image 1) the respective noisy image ($\sigma = 20$), and the denoised images obtained by N2V and by N2N methods.

TABLE I. RESULTS FOR N2N AND N2V METHODS CONSIDERING THE TEST SET, PSNR, AND RMSE METRICS ($\sigma = 20$)

Methods	PSNR	RMSE
N2N	31.1867	0.0261
N2V	24.4983	0.0596

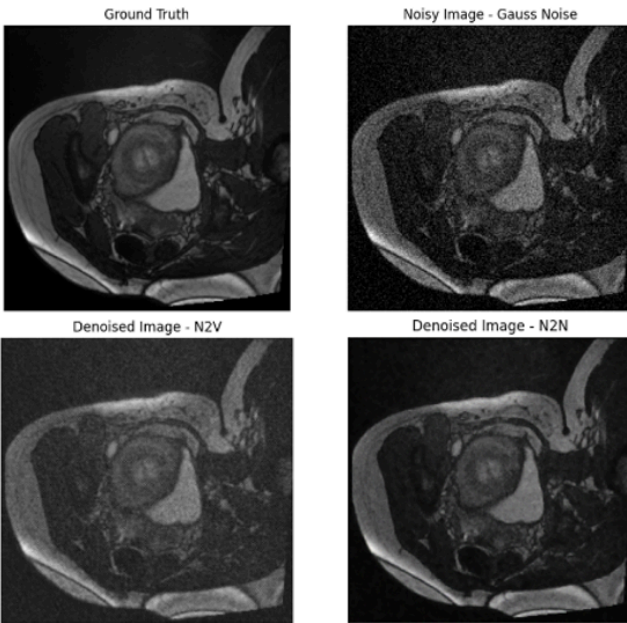


Fig. 3. Representation of one clean image (image 2) the respective noisy image ($\sigma = 20$), and the denoised images obtained by N2V and by N2N methods.

For comparison purposes, we also tested the methods with noisy images generated by Gaussian noise using $\sigma = 5$, with the hyperparameters of the networks and training/test setup remaining unchanged. The quantitative results for both methods are summarized in Table II and Fig. 4 shows a

graphic representation. For this situation, the results corroborated with the previous conclusions. In other words, the N2N was better than N2V also for this case. However, using $\sigma = 5$ to generate the noisy images, the metrics were improved for both methods, this is expected once the level of noise is reduced. In this sense, the noise that corrupts the original images is much less in this situation, as we can see in Fig. 4. Indeed, by visual analysis, it is more complicated to recognize the noise presented in the noisy image of Fig. 4 compared to the noisy images presented in both Figs 2 and 3. On the other hand, this noise may be more representative of real fetal MR images.

TABLE II. RESULTS FOR N2N AND N2V METHODS CONSIDERING THE TEST SET, PSNR, AND RMSE METRICS ($\sigma = 5$)

Methods	PSNR	RMSE
N2N	40.3567	0.0001
N2V	29.3456	0.0342

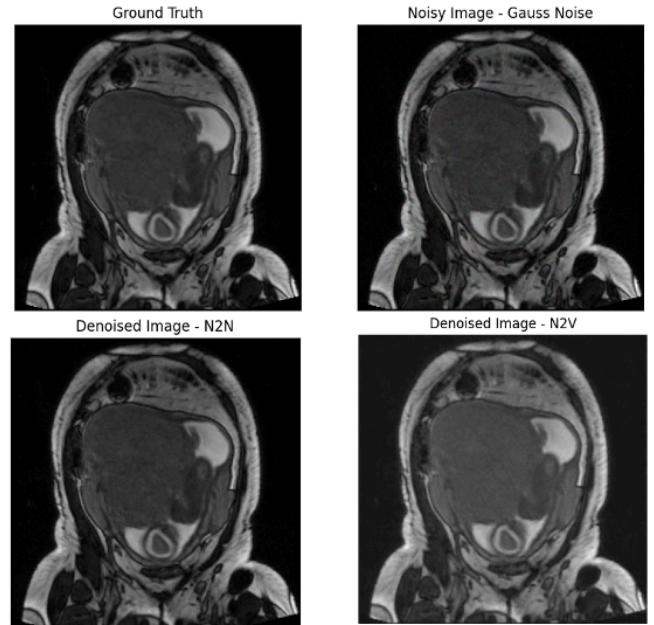


Fig. 4. Representation of one clean image (image 1) the respective noisy image ($\sigma = 5$), and the denoised images obtained by N2V and by N2N methods.

VI. CONCLUSIONS

This work aimed to apply two image denoising methods that do not require the ground truth images to train (N2N and N2V). For the tests we used a fetal MRI dataset corrupted by Gaussian noise and compared the results using visual analysis and two image quality metrics evaluation, PSNR and RMSE.

Even though the N2V was derived from N2N and had arisen as a better model than N2N, in situations without ground truth images, in this work the N2V was worse than N2N in two different tests, when noisy images were generated using $\sigma = 5$ and $\sigma = 20$ and mean equal to zero. On the other hand, both methods presented very small error ratios (RMSE) for both tests, which indicates that they are promising alternatives for image denoising tasks in the medical area.

Also, we could conclude that even with a considered small dataset to train deep models we reached good results with the applied unsupervised methods using images with two levels of noise. But we recognize that there is a place to improve the results in further works.

For future works, we intend to test more methods that do not require of ground truth images, such as deep image prior [27] and NOISE2SELF (N2S) [12] which is also derived from N2N. Besides, we want to test other types of medical images, such as ultrasonography imagery and to perform data augmentation to provide more information to the tested models and to try improve the results. Besides, we intend to test N2N and N2V for noisy images generated by different noise levels to compare the results and to perform such tests using k-fold cross-validation.

ACKNOWLEDGMENT

The authors would like to thank FAPERJ (“Fundação Carlos Chagas Filho de Amparo à Pesquisa do Estado do Rio de Janeiro”) for funding this paper (Financing Code E-26/200.640/2023 (284828)). The study involving fetal MRI was approved by the DASA ethics committee. All patients involved signed a consent form approving the use of the images used in this research.

REFERENCES

- [1] S. Kollem, K. R. Reddy, and D. S. Rao, ‘A novel diffusivity function-based image denoising for MRI medical images’, *Multimed. Tools Appl.*, Mar. 2023, doi: 10.1007/s11042-023-14457-3.
- [2] A. Lim, J. Lo, M. W. Wagner, B. Ertl-Wagner, and D. Sussman, ‘Motion artifact correction in fetal MRI based on a Generative Adversarial network method’, *Biomed. Signal Process. Control*, vol. 81, p. 104484, Mar. 2023, doi: 10.1016/j.bspc.2022.104484.
- [3] J.-J. Huang and P. L. Dragotti, ‘WINNet: Wavelet-Inspired Invertible Network for Image Denoising’, *IEEE Trans. Image Process.*, vol. 31, pp. 4377–4392, 2022, doi: 10.1109/TIP.2022.3184845.
- [4] K. Prabakaran, N. Lalithamani, and P. Kiruthika, ‘Speckle Reduction Algorithm for Medical Ultrasound Imaging’, *Asian J. Res. Soc. Sci. Humanit.*, vol. 6, no. 6, p. 148, 2016, doi: 10.5958/2249-7315.2016.00202.1.
- [5] R. S. Thakur, S. Chatterjee, R. N. Yadav, and L. Gupta, ‘Chapter 5 - Medical image denoising using convolutional neural networks’, in *Digital Image Enhancement and Reconstruction*, S. S. Rajput, N. U. Khan, A. K. Singh, and K. V. Arya, Eds., in Hybrid Computational Intelligence for Pattern Analysis. , Academic Press, 2023, pp. 115–138. doi: 10.1016/B978-0-32-398370-9.00012-3.
- [6] J. Lehtinen, J. Munkberg, J. Hasselgren, S. Laine, T. Karras, M. Aittala, and T. Aila, ‘Noise2noise: Learning image restoration without cleandata.’ in ICML, 2018.
- [7] A. Krull, T.-O. Buchholz, and F. Jug, Noise2void-learning denoising from single noisy images. Proceedings of the IEEE Computer Society Conference on Computer Vision and Pattern Recognition 2019–June:2124–2132, 2019, doi:10.1109/CVPR.2019.00223.
- [8] Y. Zharov, E. Ametova, R. Spiecker, T. Baumbach, G. Burca, and V. Heuveline, ‘Shot noise reduction in radiographic and tomographic multi-channel imaging with self-supervised deep learning’, *Opt. Express*, vol. 31, no. 16, pp. 26226–26244, Jul. 2023, doi: 10.1364/OE.492221.
- [9] R. Houhou *et al.*, ‘Comparison of denoising tools for the reconstruction of nonlinear multimodal images’, *Biomed. Opt. Express*, vol. 14, no. 7, pp. 3259–3278, Jul. 2023, doi: 10.1364/BOE.477384.
- [10] W. Jung *et al.*, ‘MR-self Noise2Noise: self-supervised deep learning-based image quality improvement of submillimeter resolution 3D MR images’, *Eur. Radiol.*, vol. 33, no. 4, pp. 2686–2698, Apr. 2023, doi: 10.1007/s00330-022-09243-y.
- [11] J. Jurek, A. Materka, K. Ludwisiak, A. Majos, and F. Szczepankiewicz, ‘Phase Correction and Noise-to-Noise Denoising of Diffusion Magnetic Resonance Images Using Neural Networks’, in *Computational Science – ICCS 2023*, J. Mikiyška, C. de Mulatier, M. Paszynski, V. V. Krzhizhanovskaya, J. J. Dongarra, and P. M. A. Sloot, Eds., in Lecture Notes in Computer Science. Cham: Springer Nature Switzerland, 2023, pp. 638–652. doi: 10.1007/978-3-031-36021-3_61.
- [12] J. Batson and L. Royer, ‘Noise2Self: Blind Denoising by Self-Supervision’, in *Proceedings of the 36th International Conference on Machine Learning*, PMLR, May 2019, pp. 524–533. Accessed: May 16, 2023. [Online]. Available: <https://proceedings.mlr.press/v97/batson19a.html>
- [13] G. Ashwini and T. Ramashri, ‘Denoising of COVID-19 CT and chest X-ray images using deep learning techniques for various noises using single image’, in *2023 International Conference on Signal Processing, Computation, Electronics, Power and Telecommunication (IConSCEPT)*, May 2023, pp. 1–6. doi: 10.1109/IConSCEPT57958.2023.10170038.
- [14] M. Lesage *et al.*, ‘An end-to-end pipeline based on open source deep learning tools for reliable analysis of complex 3D images of ovaries’, *Development*, vol. 150, no. 7, p. dev201185, Apr. 2023, doi: 10.1242/dev.201185.
- [15] S. Yun *et al.*, ‘Penalty-driven enhanced self-supervised learning (Noise2Void) for CBCT denoising’, in *Medical Imaging 2023: Physics of Medical Imaging*, SPIE, Apr. 2023, pp. 464–469. doi: 10.1117/12.2652826.
- [16] S. Kojima, T. Ito, and T. Hayashi, ‘Denoising Using Noise2Void for Low-Field Magnetic Resonance Imaging: A Phantom Study’, *J. Med. Phys.*, vol. 47, no. 4, p. 387, Dec. 2022, doi: 10.4103/jmp.jmp_71_22.
- [17] Z. Wu, X. Chen, S. Xie and Y. Zeng, ‘Super-resolution of brain MRI images based on denoising diffusion probabilistic model’, *Biomed. Signal Process. Control*, vol. 85, p. 104901, Aug. 2023, doi: 10.1016/j.bspc.2023.104901.
- [18] A. Khmag, ‘Additive Gaussian noise removal based on generative adversarial network model and semi-soft thresholding approach’, *Multimed. Tools Appl.*, vol. 82, no. 5, pp. 7757–7777, Feb. 2023, doi: 10.1007/s11042-022-13569-6.
- [19] O. Ronneberger, P. Fischer, and T. Brox, *U-Net: Convolutional Networks for Biomedical Image Segmentation*, vol. 9351. 2015, p. 241. doi: 10.1007/978-3-319-24574-4_28.
- [20] S. Ioffe and C. Szegedy, ‘Batch Normalization: Accelerating Deep Network Training by Reducing Internal Covariate Shift’. arXiv, Mar. 02, 2015. doi: 10.48550/arXiv.1502.03167.
- [21] A. Paszke *et al.*, ‘PyTorch: An Imperative Style, High-Performance Deep Learning Library’. arXiv, Dec. 03, 2019. doi: 10.48550/arXiv.1912.01703.
- [22] M. Abadi *et al.*, ‘TensorFlow: Large-Scale Machine Learning on Heterogeneous Distributed Systems’, *ArXiv160304467 Cs*, Mar. 2016, Accessed: Jul. 03, 2021. [Online]. Available: <http://arxiv.org/abs/1603.04467>
- [23] N. Ketkar, ‘Introduction to Keras’, in *Deep Learning with Python: A Hands-on Introduction*, N. Ketkar, Ed., Berkeley, CA: Apress, 2017, pp. 97–111. doi: 10.1007/978-1-4842-2766-4_7.
- [24] K. He, X. Zhang, S. Ren, and J. Sun, ‘Delving Deep into Rectifiers: Surpassing Human-Level Performance on ImageNet Classification’, *IEEE Int. Conf. Comput. Vis. ICCV 2015*, vol. 1502, Feb. 2015, doi: 10.1109/ICCV.2015.123.
- [25] D. P. Kingma and J. Ba, ‘Adam: A Method for Stochastic Optimization’. arXiv, Jan. 29, 2017. doi: 10.48550/arXiv.1412.6980.
- [26] A. Shah *et al.*, ‘Comparative analysis of median filter and its variants for removal of impulse noise from gray scale images’, *J. King Saud Univ. - Comput. Inf. Sci.*, vol. 34, no. 3, pp. 505–519, Mar. 2022, doi: 10.1016/j.jksuci.2020.03.007.
- [27] D. Ulyanov, A. Vedaldi, and V. Lempitsky, ‘Deep Image Prior’, presented at the Proceedings of the IEEE Conference on Computer Vision and Pattern Recognition, 2018, pp. 9446–9454. Accessed: May 16, 2023. [Online]. Available: https://openaccess.thecvf.com/content_cvpr_2018/html/Ulyanov_Deep_Image_Prior_CVPR_2018_paper.html